Secondary organic aerosols from anthropogenic and biogenic precursors

U. Baltensperger,*[a] M. Kalberer,[b] J. Dommen,[a] D. Paulsen,[a] M. R. Alfarra,[ac] H. Coe,[c] R. Fisseha,[a] A. Gascho,[a] M. Gysel,[ac] S. Nyeki,[a] M. Sax,[b] M. Steinbacher,[a] A. S. H. Prevot,[a] S. Sjögren,[a] E. Weingartner[a] and R. Zenobi[b]

[a] *Laboratory of Atmospheric Chemistry, Paul Scherrer Institut, 5232, Villigen, Switzerland*
[b] *Department of Chemistry and Applied Biosciences, ETH Zurich, 8093, Zurich, Switzerland*
[c] *School of Earth, Atmospheric and Environmental Sciences, The University of Manchester, P. O. Box 88, Manchester, UK, M60 1QD*

Received 16th November 2004, Accepted 7th February 2005

Secondary organic aerosol (SOA) formation from the photooxidation of an anthropogenic (1,3,5-trimethylbenzene) and a biogenic (α-pinene) precursor was investigated at the new PSI smog chamber. The chemistry of the gas phase was followed by proton transfer reaction mass spectrometry, while the aerosol chemistry was investigated with aerosol mass spectrometry, ion chromatography, laser desorption ionization mass spectrometry, and infrared spectroscopy, along with volatility and hygroscopicity studies. Evidence for oligomer formation for SOA from both precursors was given by an increasing abundance of compounds with a high molecular weight (up to 1000 Da) and by an increasing thermal stability with increasing aging time. The results were compared to data obtained from ambient aerosol samples, revealing a number of similar features.

Introduction

Ambient aerosol particles have a variety of important impacts, including adverse health effects, visibility reduction and their influence on climate. Carbonaceous aerosols are a major component of the total aerosol mass and can account for up to 50% of the fine particulate mass concentration ($PM_{2.5}$) on an annual average. However, their concentrations, size distribution and formation mechanisms are less understood than those of other compounds such as sulfate and nitrate. An excellent review on the current state of knowledge of organic aerosol is given by Kanakidou *et al.*[1]

The formation of secondary organic aerosols (SOA) has recently received much attention. Many natural volatile organic compounds (VOC) like terpenes or sesquiterpenes, as well as aromatic VOCs, which are mainly of anthropogenic origin, have been found to be precursors of SOA. Aromatics are emitted by fuel combustion and evaporation and will therefore influence SOA formation mainly in polluted urban areas. SOA is formed when the biogenic and anthropogenic precursor species react with atmospheric oxidants such as hydroxyl radicals, ozone, and nitrogen oxide species. Even in urban areas, up to 90% of the total organic aerosol mass can be attributed to

DOI: 10.1039/b417367h

SOA.[2] However, natural aerosol formation processes are also strongly influenced by human-induced atmospheric composition change since increased oxidant levels can enhance the natural aerosol production.[3]

Efforts have been made to quantify the aerosol formation potential (aerosol yield) of both terpenes and aromatic compounds. Odum *et al.*[4] showed that the aerosol yield of whole gasoline vapor can be explained by the sum of the single SOA yields of its aromatic constituents. Most models describing SOA formation assume a thermodynamic equilibrium of organic compounds between the gas and the aerosol phase. However, these models underestimate the organic partitioning into the aerosol phase of many compounds (*e.g.* Jang *et al.*[5]).

The composition of SOA on the molecular level is difficult to analyze, and studies conducted so far were only able to resolve a small fraction of the entire organic particle mass.[6] Therefore, approaches based on functional group analysis have been applied, which revealed the general structure of the organic mass.[7]

Low molecular weight compounds that are expected to be highly volatile have been found in secondary organic aerosol by various authors.[8–11] It was speculated that these species might actually be formed by decomposition of larger, less volatile molecules during the analysis[10] and that polyketones formed from photooxidation of toluene may be present as polymers rather than monomers.[11] Jang *et al.*[5] used chamber studies to show that some of the highly volatile carbonylic oxidation products (expected to be mostly in the gas phase) can lead to an increase of SOA mass if mixed with strongly acidic inorganic seed particles. They proposed acid catalyzed condensation and polymerization reactions of carbonyls in the acidic particles as a possible explanation of the observed SOA mass increase. Limbeck *et al.*[12] showed that secondary aerosol formation of atmospheric polymers occurs by heterogeneous reaction of isoprene and terpenoids in the presence of a sulfuric acid aerosol catalyst.

The terms polymerization and oligomerization have been interchangeably used in aerosol science literature for the process of converting a monomer or a mixture of monomers into a molecule of higher relative molecular mass. The definitions given by the International Union of Pure and Applied Chemistry (IUPAC) (http://www.iupac.org/reports/1996/6812jenkins/alphaterm.html) are in short, the following:

- Polymer molecule: A molecule of high relative molecular mass, the structure of which essentially comprises the multiple repetition of units derived from molecules of low relative molecular mass. A molecule can be regarded as having a high relative molecular mass if the addition or removal of one or a few of the units has a negligible effect on the molecular properties.
- Oligomer molecule: Similar structure as a polymer molecule but only of intermediate relative molecular mass, whereby its properties do vary significantly with the removal of one or a few of the units.
- Polymerization: The process of converting a monomer or a mixture of monomers into a polymer.
- Oligomerization: The process of converting a monomer or a mixture of monomers into an oligomer.

As shown below the relative molecular mass of macromolecules found in aerosols is on the order of a few hundred Dalton. Thus, these macromolecules are comprised of only a few monomer units. Therefore, oligomerization might be the more appropriate term for this reaction in the aerosol forming oligomers. We use this terminology in the following text.

The hypothesis of oligomerization reactions has recently been corroborated by new experiments. Iinuma *et al.*[13] and Tolocka *et al.*[14] investigated aerosol formation from α-pinene ozonolysis in the presence of acid seed particles and observed the formation of compounds with molecular mass higher than 300 Da. Some masses could be attributed to combinations of known primary products of this reaction. Both aldol condensations and gem-diol reactions were suggested as possible pathways for oligomer formation. Kalberer *et al.*[15] analyzed SOA formed from the photooxidation of an aromatic compound (1,3,5-trimethylbenzene) in the presence of NO_x and found oligomeric compounds up to $m/z = 1000$. Kleindienst *et al.*[16] confirmed the formation of multi-functional oxygenates in the photooxidation of toluene, with many of these compounds being present both in the gas and the particle phase. Moreover, evidence was found for a series of multifunctional acids produced as higher order oxidation products. Koehler *et al.*[17] also reported SOA formation by reactive condensation of volatile furandiones and aldehydes.

Recent findings also indicate that a significant SOA fraction might originate from other compounds such as isoprene, which has been believed for the last decade to produce little aerosol mass.[18,19] Claeys *et al.*[20,21] showed that a range of isoprenoid-like polyols were present in the Amazonia. The presence of these species could be explained by OH initiated photo-oxidation of isoprene. Claeys *et al.*[20,21] calculated that these polyols could explain between 5 and 25% of the global biogenic contribution to secondary organic aerosol. Isoprene is estimated to account for 44% of total emitted biogenic VOC emissions and amounts to about 4 times the mass of anthropogenically emitted VOCs (http://geiacenter.org/index.html).

Other processes may also lead to molecules of high relative molecular mass. Hoffer *et al.*[22] showed that a representative lignin-type component from biomass burning aerosol reacts with OH radicals in model cloud water yielding colored organic species. They provided experimental evidence that actually larger molecular weight species are formed in the aqueous phase by free radical oligomerization.

Such oligomers have been previously identified in several field studies on atmospheric aerosols, and due to their similarities with humic acids (*e.g.*, high molecular weight, hygroscopic properties, *etc.*), are commonly known as HULIS (humic-like substances).[23,24] Such compounds can make up to 30% of the organic aerosol fraction of the atmospheric aerosol.[25,26] As it was recognized that these HULIS were not soil-derived (*e.g.* based on their predominance in the submicrometre fraction of the aerosol), their origin was the subject of highly diverse speculation.

Kleindienst *et al.*[16] found products in the ambient environment having nearly the same mass spectrum as in smog chamber studies of toluene photooxidation. These products contained multiple acid and alcoholic-OH moieties. They had a substantially lower volatility than previously reported SOA products of the toluene photooxidation and might serve as an indicator for aromatic oxidation in the ambient atmosphere.

This paper provides a detailed chemical and physical characterization of SOA particles generated in a smog chamber from anthropogenic and biogenic precursors. Experimental evidence is given that the chemical composition of SOA particles changes substantially over an extended period of time, even after the physical growth levels out. Results showing the continuous oxidation and oligomerization of the particle bulk are presented.

Experimental

Secondary organic aerosol formation was investigated in the new smog chamber at PSI. A detailed description of the chamber is found in Paulsen *et al.*[27] The chamber is a 27-m^3 (3 × 3 × 3 m) flexible bag made of 125 μm DuPont™ *Teflon*® fluorocarbon film (FEP, type 500A, Foiltec GmbH, Germany). The bag is suspended in a temperature controlled wooden enclosure of dimension 4 × 5 × 4 m (L × W × H). The walls, floor and ceiling of the enclosure are covered with reflective aluminum foil to maximize the light intensity and increase light scatter or diffusion. The chamber temperature is controlled by two cooling units allowing for temperature stabilization of ±1 °C within the range of 15 to 30 °C. Two manifolds (inlet and outlet) made of stainless steel and *Teflon*® allow for easy installation of additional inputs and sampling lines.

Four xenon arc lamps (4 kW rated power, 1.55×10^5 lumens each, XBO® 4000 W/HS, OSRAM) are used to simulate the solar light spectrum and to mimic natural photochemistry. The light is filtered with borosilicate glass plates to reduce the high actinic UV below the wavelength of 300 nm. A NO_2 photolysis rate of $J_{NO_2} = 2 \times 10^{-3}\ s^{-1}$ is obtained.

Purified air is supplied by an AADCO (737-250 series, AADCO Instruments, Inc., USA) pure air generation system. An ozone generator is provided by irradiation of pure air in quartz tubes with UV lamps generating ozone of ppbv to ppmv mixing ratios in the chamber. Liquid parent hydrocarbon is evaporated in a heated 500 ml glass sampling bulb. The humidification system uses a commercial clothes steamer (J-4000 series, Jiffy® Steamer Company, LLC, USA). Table 1 gives an overview of the available analytical instrumentation. More information on the chemical and physical techniques used to analyze the oxidized gaseous and particle reaction products is found elsewhere.[15,27–32]

In the experiments presented here, 1,3,5-trimethylbenzene (TMB) as well as α-pinene were used as SOA precursors. Standard conditions were in the case of TMB: 600 ppbv 1,3,5-TMB, 150 ppbv NO, 150 ppbv NO_2, and 300 ppbv propene at 50% RH, and in the case of α-pinene: 160 ppbv α-pinene,

Table 1 List of analytical instruments at the PSI smog chamber

Instrument	Monitored parameter
Rotronic Hygro Clip SC05 humidity sensor	Relative humidity (RH, %), temperature
Thermocouple type K	Chamber temperatures
Vaisala PTA 427 pressure transmitter	Ambient pressure
Aero Laser 5002	Carbon monoxide (CO)
Environics S300 ozone analyzer	Ozone (O_3)
Monitor Labs 9841A NO_x analyzer	Oxides of nitrogen (NO and NO_x-NO)
Monitor Labs 8810 ozone analyzer	Ozone (O_3)
Proton transfer mass spectrometer (PTR-MS)	Volatile organic compounds
Thermo Environmental Instruments 42C trace level NO_x analyzer	Oxides of nitrogen (NO and NO_x-NO)
Gas chromatography-mass spectrometry (GC-MS) together with PUF/Filter or denuder sampling	Organic compounds
Impactor for laser desorption ionization-mass spectrometry LDI-MS) and Fourier transform infrared spectroscopy (FTIR)	Organic compounds
Condensation particle counter (CPC, TSI 3022)	Total particle number concentration
Condensation particle counter (CPC, TSI 3025)	Total particle number concentration
Scanning mobility particle sizer (SMPS, TSI 3071 and 3010 CPC)	Number weighted particle size distribution
Wet effluent diffusion denuder/ aerosol collector (WEDD/AC) along with ion chromatography coupled to mass spectrometry (partly)	Inorganic and organic acids in gas and aerosol phase
Volatility tandem differential mobility analyzer (VTDMA)	Particle volatility
Hygroscopicity tandem differential mobility analyzer (HTDMA, partly)	Particle hygroscopicity
Aerodyne aerosol mass spectrometer (AMS, partly)	Size resolved chemical composition

65 ppbv NO, 65 ppbv NO_2, and 300 ppbv propene at 50% RH. All experiments were performed without preexisting seed particles. Overall, the experiments were characterized by a high reproducibility both for the gas and aerosol phase.[27]

Results

Fig. 1 presents PTR-MS mass traces for the dry clean air (Panel A), humidified clean air (Panel B), the reactant mixture before starting the irradiation (Panel C), and 2.5 h after starting the irradiation of a TMB-propene-NO_x-water vapor mixture (Panel D). Panel A demonstrates the good performance of the clean air generator, with a good background of mostly less than 15 counts s^{-1} (cps) corresponding to the noise level of the instrument. A few peaks are present, probably due to some off-gassing from the chamber wall. These peaks also appear as products during the photooxidation experiments, the highest of which belong to acetaldehyde (*m*/*z* 45, protonated ion is observed), formic acid (*m*/*z* 47), and acetic acid (*m*/*z* 61). It should however be noted that peak assignment based on PTR-MS results may be ambiguous, since only the molecular weight is known.

When transporting and transferring the water from the Milli-Q Academic ultrapure water system (18.2 MΩ cm at 25 °C; 5–10 ppbv total organic carbon, Millipore, USA) care was taken to reduce outside contamination, for example, from the ambient atmosphere. Despite of this care, most peaks already visible in dry air increase after the addition of water. Based on this we assume that these compounds are not caused by water contamination but may also be volatilized from the bag wall after humidification (as it is well known *e.g.* for nitrous acid). The increase of the mass peaks *m*/*z* 55 and 73 comes from increased water clustering at higher humidity. After irradiation, about 50 mass peaks are formed, of which about 15 have so far been identified based on literature data. The

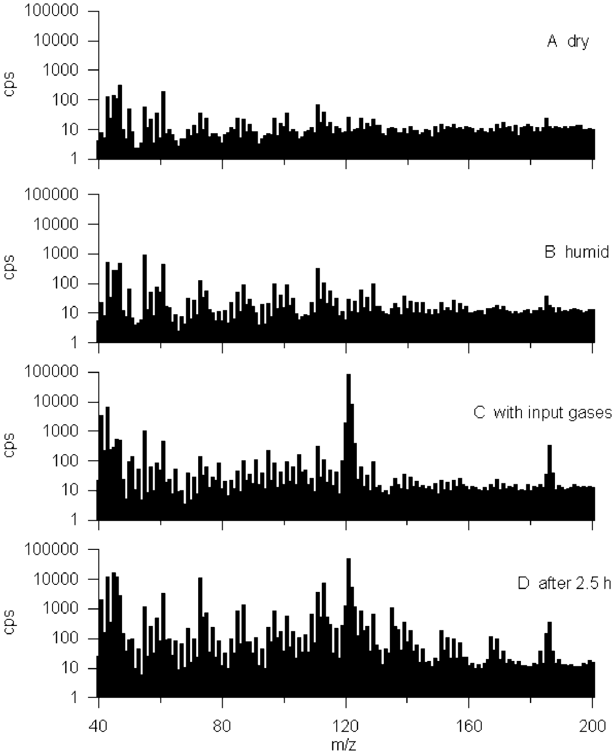

Fig. 1 PTR-MS spectra for the dry clean air (Panel A), humidified clean air (Panel B), the reactant mixture (nominally 1200 ppb 1,3,5-TMB, 320 ppb NO, 320 ppb NO_2, and 300 ppb propene at 50% RH) before starting the irradiation (Panel C), and 2.5 hours after starting the irradiation (Panel D).

strongest signals arise from acetaldehyde (*m*/*z* 45), formic acid (*m*/*z* 47), acetic acid (*m*/*z* 61), methylglyoxal (*m*/*z* 73), 2-methyl-4-oxo-2-pentenal and 3,5-dimethyl-5(2H)-2-furanone (*m*/*z* 113), and 3,5-dimethyl-benzaldehyde (*m*/*z* 135).

Fig. 2 shows the development of oxidized organic reaction products during a TMB photo-oxidation experiment. The acids were measured with the WEDD-AC IC system. Mass traces recorded by PTR-MS have been grouped into sum-1, sum-2 and sum-3 depending on their temporal concentration profile. Thus, sum-1 and sum-2 comprise all mass traces which increase sharply 20–30 min after the experiment start and reach a maximum after about 150 or 300 min, respectively. Mass traces increasing late in the experiment and continuing to rise throughout are included in sum-3. Mass peaks of organic acids were excluded from these groups since they experience losses in the inlet of the PTR-MS system. Thus, sum-1, sum-2 and sum-3 probably consist mostly of carbonylic compounds. The sum of eight acids as measured by the WEDD-AC IC increases over the whole experiment time. These compounds appear rather late in the experiment significantly increasing only after about 100 min, similarly to sum-3 from PTR-MS. The acids and the compounds of sum-3 seem to be secondary or later oxidation products of the oxidation chain. On the other hand compounds comprised in sum-1 and sum-2 are formed early in the oxidation scheme. They decrease later on due to a reduced formation rate combined with loss due to further reaction with OH radicals and photolysis. The observed particle nucleation (particle diameters $D > 3$ nm as measured with a CPC 3025, TSI) starts after about 15–20 min, and it may be speculated that compounds formed early in the oxidation scheme might be involved in the nucleation process rather than the low-volatility acids.

After approximately 25 minutes of irradiation, particle formation is detectable by the SMPS. Fig. 3 shows time resolved number weighted particle size distributions formed from the irradiation

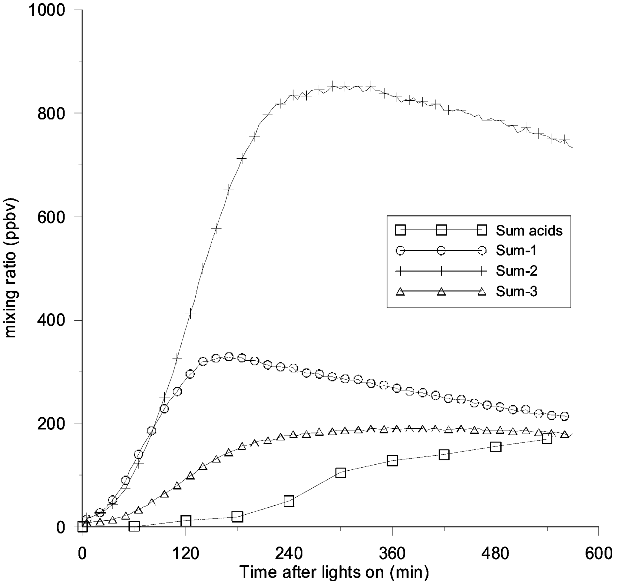

Fig. 2 Mixing ratio *vs.* time for the sum of eight acids measured with the WEDD-AC IC and three groups of mass traces from PTR-MS selected according to their temporal profile.

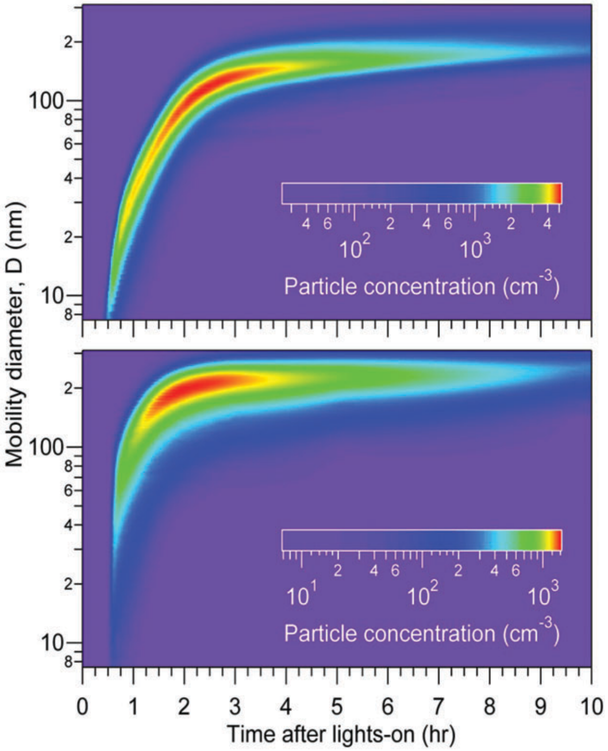

Fig. 3 Size distribution evolution of secondary organic aerosol. Top panel: 1,3,5-TMB/NO_x/C_3H_6 (650 ppbv/320 ppbv/300 ppbv initial mixing ratios) at 50% RH; bottom panel: α-pinene/NO_x/C_3H_6/H_2O (160 ppbv/130 ppbv/300 ppbv initial mixing ratios) at 50% RH.

Table 2 Organic acids identified both in the gas and aerosol phase at the maximum aerosol concentration (4 h 30 min after lights on) (NQ: not quantified; NI: not identified; NP: not present). Last column: acids identified in ambient aerosol filter samples from downtown Zurich

			Gas phase	Aerosol phase		
Mass	Compound	Type (IC-MS)	Conc/μg m^{-3} (IC-MS)	Conc/μg m^{-3} (IC-MS)	Vol. ratio (IC-MS)	Found in atmospheric samples (Zurich)
46	Formic acid	Mono	75.2	15	0.07	Yes
60	Acetic acid	Mono	26.1	16	0.08	Yes
88	Pyruvic acid	Mono	29.2	11	0.05	Yes
90	Lactic acid	Mono	43.8	44	0.21	Yes
90	Oxalic acid	Di	0.26	0.42	0.001	Yes
104	Malonic acid	Di	NQ	N.Q	—	No
114	NI	Di	NQ	N.Q	—	No
118	Succinic acid	Di	0.54	0.49*	0.006	Yes
122	NI	Di	NQ	NP	—	Yes
129	NI	—	NQ	N.Q	—	No
130	Methyl maleic acid	Di	25.6	0.4	0.001	Yes
132	NI	Di	NQ	N.Q	—	Yes
134	Malic acid	Di	0.4*	0.23*	0.001	Yes
150	3,5-Dimethylbenzoic acid	Mono	NP	N.P	—	?
166	NI	Di	0.04	0.10	0.0005	Yes
171	NI	—	NQ	N.Q	—	No
178	NI	Di	NQ	N.Q	—	Yes
188	NI	Di	0.03	0.12	0.0005	?
190	NI	Di	NQ	N.Q	—	?
192	Citric acid	Tri	0.03	0.03	0.0003	No
234	NI	Di	NQ	10.9	0.05	No

of 1,3,5-TMB-propene-NO_x-H_2O and α-pinene-propene-NO_x-H_2O (data not corrected for wall losses). In general, particle formation from α-pinene occurs later, but is then followed by a higher growth rate, resulting in significantly larger particles.

Correction of wall losses was then performed by fitting the decrease of the integrated particle number concentrations over time to an exponential decay function.[27] Volume concentrations were calculated from the corrected number size distributions assuming spherical shape. From the volume concentrations, mass concentrations were calculated using densities of 1.37 for TMB SOA and 1.30 for α-pinene SOA.[32] These densities had been calculated by simultaneous measurements of the mobility diameter (with the SMPS) and the vacuum aerodynamic diameter measured in the free molecular regime with the AMS.[33] The aerosol yield was then determined according to:

$$Y = \frac{\Delta M_o}{\Delta \mathrm{ROG}} \tag{1}$$

where ΔM_o/μg m^{-3} is the organic aerosol mass concentration produced for a certain amount of reacted organic gas (ROG), ΔROG/μg m^{-3}.[4]

For an initial mixing ratio of 600 ppbv TMB, the average aerosol yield was 7.7 ± 2.1% after accounting for losses.[27] This value falls within the range of wall loss corrected yields reported by Cocker *et al.*[34] of 3.4 to 8.1% for experiments without seed particles having the same parent organic hydrocarbon at similar input conditions.

A closer look at the chemistry of TMB SOA with GC-MS revealed that several of the small carbonyls found in the gas phase (methylglyoxal, 2-methyl-4-oxo-2-pentenal, and about ten unidentified carbonyls) as well as a number of organic acids were found in the particle phase. Even more organic acids (in total about 20) were identified with IC-MS (Table 2).[29] Table 2 also shows that most of the acids found in the TMB SOA are also present in the ambient aerosol sampled in downtown Zurich.

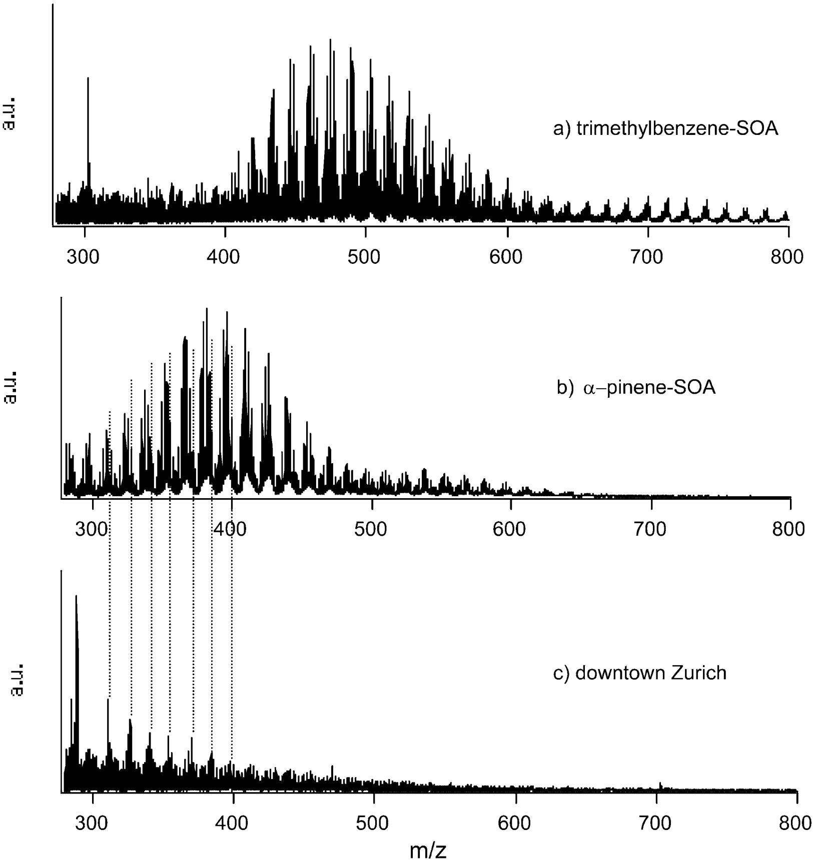

Fig. 4 Comparison of LDI-MS spectra for TMB-SOA, α-pinene-SOA, and ambient aerosol from downtown Zurich between *m/z* 280–800.

Kalberer *et al.*[15] showed that laser desorption/ionization mass spectrometry (LDI-MS) is well suited to demonstrate the increasing degree of oligomerization (with molecular weights up to 1000 Da) with SOA aging time. Fig. 4 presents LDI-MS spectra of SOA from TMB and α-pinene, as well as from an atmospheric aerosol sample obtained in the city of Zurich. The temporal evolution and the general structure of the oligomer mass spectra are similar for different precursors, with dominant mass differences of *m/z* 14 or *m/z* 16 between about *m/z* 400–800 and 250–650, for TMB and α-pinene, respectively (Fig. 4a,b). The repetitive Δ*m/z* 14 and Δ*m/z* 16 units are shifted for the SOA oligomer from TMB compared to the oligomer structure from α-pinene. In both cases the molecular weight of the oligomers seems to reach a limit of about *m/z* 800 and *m/z* 650 for TMB and α-pinene, respectively. After about 7–10 hrs, mass spectra do not show a further increase of the molecular mass distribution. Fig. 4c shows a mass spectrum from water-soluble organic matter extracted from a filter, which was collected in downtown Zurich at an urban background site. Superimposed on a complex background is a similar repetitive structure between *m/z* 200–450 which is similar to that observed in the mass spectrum of α-pinene.

LDI-MS results clearly show the increasing abundance of high molecular weight compounds, however, it is difficult to quantify their abundance relative to the total mass. Quantification of the oligomer fraction was performed with a volatility tandem differential mobility analyzer (VTDMA), based on size reduction of the aerosol due to evaporation at different temperatures. Kalberer *et al.*[15] and Paulsen *et al.*[30] have shown the remaining volume after thermal treatment at 100, 150 or 200 °C to monotonically increase with aging time. About 50% of the particle mass consisted of oligomers after aging for more than 20 hours in both the TMB and α-pinene-formed SOA. It is interesting to

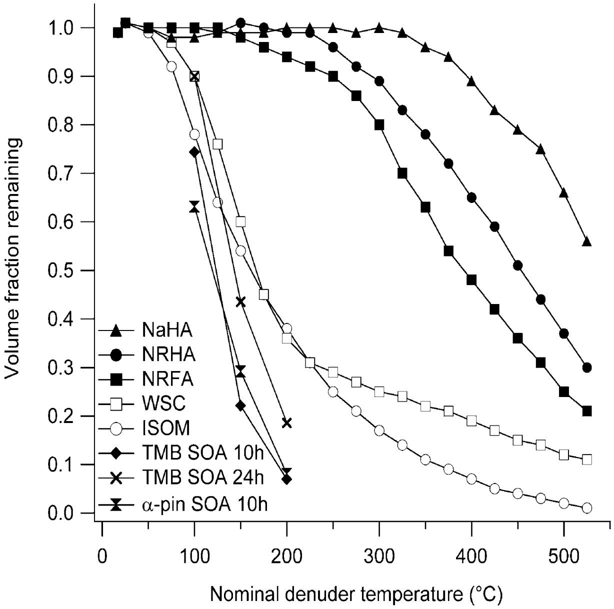

Fig. 5 Comparison of volatility curves for SOA from TMB photooxidation after 10 and 24 h, and from α-pinene after 10 h, as well as for NRHA, NRFA (Nordic reference humic and fulvic acids), NaHA (Aldrich sodium humic acid). Atmospheric aerosol samples of isolated organic matter (ISOM) and water soluble compounds (WSC) were collected at the K-puszta GAW rural station, Hungary.[38]

note that this continued decrease of the volatility is not reflected in the LDI-MS spectra, where no further growth of the oligomers is seen after 7–10 h, see above. The reason for this observation remains to be elucidated. Fig. 5 compares remaining volumes of TMB SOA and α-pinene SOA with isolated organic matter (ISOM) and water soluble compounds (WSC) from atmospheric aerosol samples collected at the K-puszta Global Atmosphere Watch rural station, Hungary, as well as with reference substances (Nordic, reference humic and fulvic acids (NRHA, NRFA) and Aldrich sodium humic acid (NaHA)).

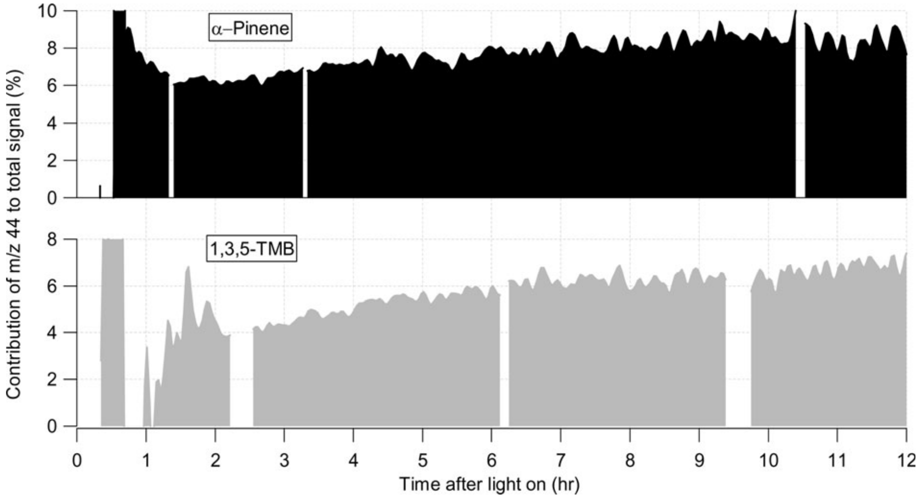

Fig. 6 Change in the relative abundance of mass 44 with time for SOA from α-pinene (top panel) and TMB (bottom panel).

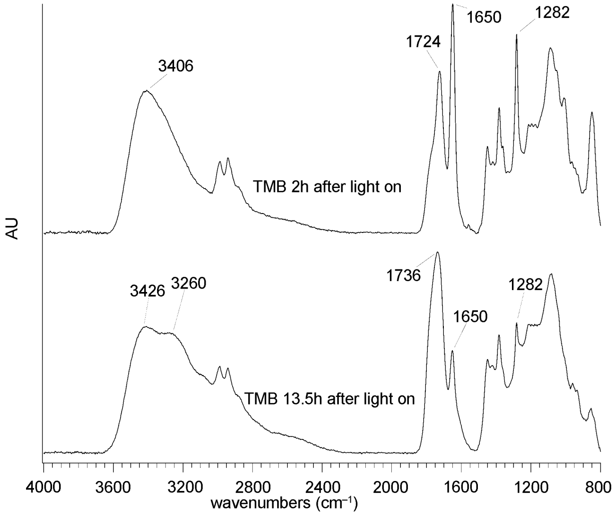

Fig. 7 FTIR spectra of TMB SOA 2 and 13.5 h after starting the irradiation.

Aerosols remaining above $T = 300$ °C are commonly attributed to refractory components such as soot, sea salt and dust. However, ISOM and WSC curves show that a substantial volatile fraction still exists in the range T = 300–525 °C, which suggests that the conventional interpretation of refractory aerosols is not valid here. However, the reference substances appear to exhibit continued volatile properties above the instrumental temperature limit at T = 525 °C. Although ISOM is similar to humic substances with respect to most properties (elemental composition, UV and fluorescence spectroscopy, IR spectroscopy, chromatographic behavior), this is not reflected here in terms of aerosol volatility. ISOM may thus be composed of less refractory compounds than humic substances, and implies a lower degree of polymerization in HULIS than in the reference humic substances that were used here.

An Aerodyne aerosol mass spectrometer (AMS)[33,35] was also used to probe both the TMB and α-pinene systems. The AMS employs a 70 eV electron impact ionization (EI), which causes a significant fragmentation of the molecules and as a result the observed polymeric signatures are weak. The EI mass spectra provide information on the chemical functionality of the sampled particles, as different ions arise from certain functional groups.[36] In these experiments both

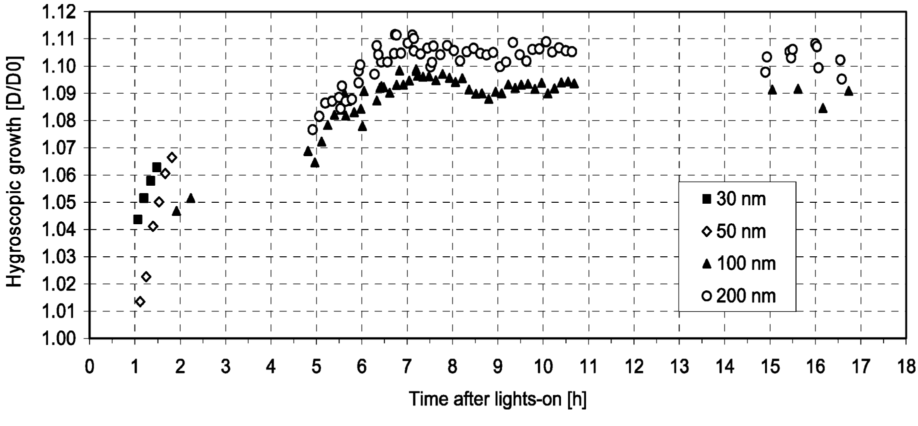

Fig. 8 Temporal evolution of the hygroscopic growth of TMB SOA at RH = 85% for four different dry particle diameters (D_0 30 to 200 nm). During the gap in the data between 11 and 15 h humidograms over the full RH range were recorded (see Fig. 9).

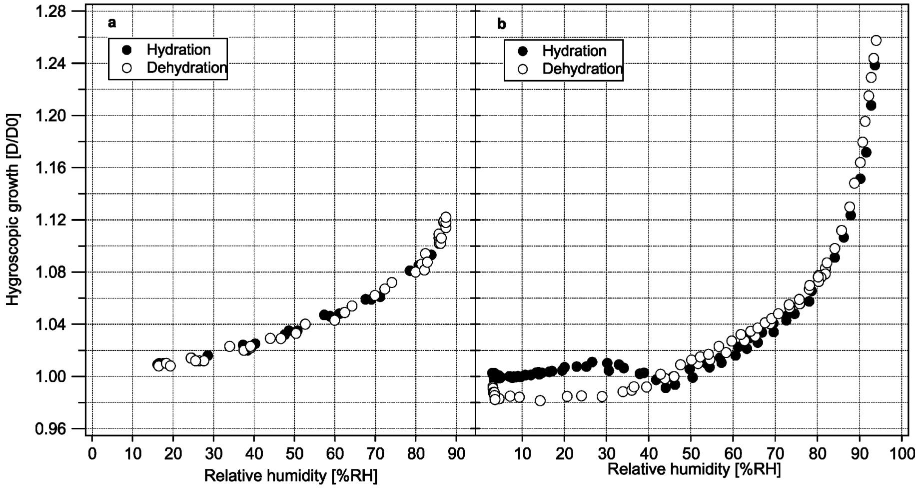

Fig. 9 Comparison of hygroscopic growth curves for TMB SOA (a) and humic-like substances isolated from K-puszta aerosol (b).

precursors produce SOA with broadly similar chemical functionality of a highly oxidized nature that is dominated by carbonyl and carboxylic acid groups, though their precise molecular composition differs.[28] The overall structure of the mass spectra measured in either experiment changed little with time, indicating that the initial molecular structure of the SOA and the SOA present much later in the experiment are not chemically dissimilar, indicating that the SOA mass increase occurs through oligomerization of monomers rather than subsequent chemical change of the initial SOA. However, some key mass fragments do increase substantially over time, such as m/z 44, indicative of hydrogen bonded acid groups, and this may indicate that increasing oxidation with time occurs (Fig. 6). Though the mass spectra of either system were not identical to that measured in the background atmosphere, the results revealed that the mass spectral signature of the photo-oxidation products of α-pinene more closely resembles the atmospheric SOA commonly observed.[28]

The increase of oxidized compounds is also observed with FTIR.[31] Fig. 7 shows FTIR spectra from TMB-SOA for 2 and 13.5 h after the start of the experiment, respectively. The OH band at 3406 cm^{-1} is clearly increasing over this time period with a second peak at 3260 cm^{-1} evolving. The OH vibration from carboxylic acids below 3200 cm^{-1} broadens with time, almost to 2400 cm^{-1}. The $C{=}O$ band at 1724 cm^{-1} is significantly broadened showing the increasing abundance of carboxylic acids and carbonyls in the aerosol. In contrast, the peaks at 1650 cm^{-1} and 1282 cm^{-1}, tentatively assigned to organonitrates, have substantially decreased in height. The same general feature is visible for α-pinene SOA (spectra not shown).

A hygroscopicity tandem differential mobility analyzer (HTDMA) was used to measure SOA hygroscopicity, *i.e.* the diameter growth factor $D(\text{RH})/D_0$ as a function of relative humidity compared to the dry diameter D_0. TMB-SOA hygroscopicity shows an increase during the first 7 h (Fig. 8) and appears to be constant after this time. Others have also reported an increasing SOA hygroscopicity in the first few hours after the start of the experiment, followed by little or no change in the growth factors for the photooxidation of *m*-xylene and TMB[34] and for the ozonolysis of α-pinene.[37]

Fig. 9a presents humidograms of TMB-SOA over an RH range of 15 to 87%. It is interesting to note that no efflorescence is seen, *i.e.* there is no difference between the hydration and dehydration curves indicating that the aerosol is still present as a supersaturated solution at 15% RH. The shape of the curves highly resemble the one obtained for humic-like substances isolated from atmospheric aerosol samples (Fig. 9b),[38] with the exception that the humic-like substances do show efflorescence, in contrast to the TMB-SOA. However, this apparent difference between SOA and humic-like substances may arise from different drying levels prior to the hydration measurement in the two experiments.

The experimental evidence shows that the aerosol mass growth slows considerably after 4–5 h while the chemical properties of the particle bulk are constantly and substantially changing over a period of more than 10 h. Hygroscopic growth factors appear to be constant after an increase during the first 7 h, while the volatility analysis shows that the oligomerization process continues at least for 28 h.[30] Unfortunately, the other measurements so far have not been sensitive enough to detect a significant change in chemistry to continue after 12 h and need to be repeated with higher sensitivity.

Conclusions

These studies indicate that the SOA formation pathway presented here is one of the major sources (though probably not the only one) of HULIS. In contrast to earlier experiments *e.g.* by Jang *et al.*,[5] oligomerization proceeds here without pre-existing strong acids on seed particles, and only with acids present in the system that were formed during the photo-oxidation. Acids formed in the photo-oxidation are thus believed to be present in sufficiently high concentrations to catalyze polycondensation or polyaddition reactions. These measurements show that oligomerization in atmospheric aerosols also takes place without acidic seed particles and under a wide range of atmospheric conditions. These findings have a number of implications for SOA modeling.[15] Current models estimating the SOA mass formation assume a thermodynamic equilibrium of gaseous oxidation products between the gas phase and the particle phase.[4,34,39] However, the uncertainty in the specific partitioning parameters may result in huge discrepancies. A recent comparison of SOA models found predicted SOA concentrations to vary by a factor of 10 or more, where the partitioning parameters were a key difference.[40] In other sensitivity studies, reducing the saturation concentrations for all precursors by a factor of 10 increased the predicted SOA mass more than twice, while with a fixed equilibrium gas mixing ratio of 2 ppt the total SOA concentration went up by a factor of three to four.[41] The latter had been used in early SOA modeling[19] and was regarded as an upper limit estimate for SOA formation. Model results with low vapor pressure will also yield diurnal variations that are more similar to measurements, with the maximum concentration in the afternoon,[42] while high vapor pressure data tend to result in a minimum in the afternoon, when temperature is highest.[43]

Oligomerization might present a reason for the fact that particulate organic carbon concentrations appear to be significantly higher than estimated based on aerosol yield determinations: oligomerization results in a substantially higher aerosol partitioning for otherwise highly volatile species such as carbonyls. In this way, gaseous compounds that have until now been considered as non-relevant for aerosol formation might contribute a substantial amount to secondary aerosol, thus explaining the missing yields found in the analysis of field experiments.[44] One important SOA precursor in this respect might be isoprene, as discussed in the introduction.

Consequently, modeling studies addressing mechanistic aspects of SOA formation may need to reconsider the current assumptions based on the oligomerization reactions described here. While the concept of two different vapor pressures for lumped compounds[45] might still be applicable, current interpretations of the model parameters might need to be revised. Revised models will result in higher SOA yields, especially at higher temperature, and with different temperature dependence. Further experiments are needed to explore the absorption behavior of the high volatility gaseous fraction into the oligomer fraction in the aerosol. Moreover, it can be expected that these oligomerization reactions affect a number of other aerosol properties such as optical parameters, hygroscopic growth, and cloud condensation nuclei potential, which are crucial to the role of aerosols in the global climate system.

Acknowledgements

This work was supported by the Swiss National Science Foundation (No. 2169-061393), by ETHZ (No. TH-10./01-2), as well as by the European Commission (EUROCHAMP, No. FP6-505968) and the Swiss Bundesamt für Bildung und Wissenschaft (ACCENT, No. 03.0430-1; EU No. GOCE-CT-2004-505337). We thank Gyula Kiss and Zoltan Krivacsy (Univeristy of Veszprem, Hungary) for providing the isolated K-puszta aerosol samples. The AMS was purchased through research grant GR3/12499 and maintained through the NERC-National Centre for Atmospheric Science (NCAS)

Universities Facility for Atmospheric Measurement (UFAM). Further support for the AMS was provided by NERC research grant NER/A/S/2003/00541.

References

1 M. Kanakidou, J. H. Seinfeld, S. N. Pandis, I. Barnes, F. J. Dentener, M. C. Facchini, R. van Dingenen, B. Ervens, A. Nenes, C. J. Nielsen, E. Swietlicki, J. P. Putaud, Y. Balkanski, S. Fuzzi, J. Hjorth, G. K. Moortgat, R. Winterhalter, C. E. L. Myhre, K. Tsigaridis, E. Vignati, E. G. Stephanou and J. Wilson, *Atmos. Chem. Phys. Discuss.*, 2004, **4**, 5855.

2 H.-J. Lim and B. J. Turpin, *Environ. Sci. Technol.*, 2002, **36**, 4489.

3 M. Kanakidou, K. Tsigaridis, F. J. Dentener and P. J. Crutzen, *J. Geophys. Res.*, 2000, **105**, 9243.

4 J. R. Odum, T. P. W. Jungkamp, R. J. Griffin, R. C. Flagan and J. H. Seinfeld, *Science*, 1997, **276**, 96.

5 M. Jang, N. M. Czoschke, S. Lee and R. M. Kamens, *Science*, 2002, **298**, 814.

6 J. H. Seinfeld and S. N. Pandis, *Atmospheric Chemistry and Physics of Air Pollution*, Wiley, New York, 1998.

7 S. F. Maria, L. M. Russell, B. J. Turpin and R. J. Porcja, *Atmos. Environ.*, 2002, **36**, 5185.

8 H. J. L. Forstner, J. H. Seinfeld and R. C. Flagan, *Environ. Sci. Technol.*, 1997, **31**, 1345.

9 H. J. L. Forstner, J. H. Seinfeld and R. C. Flagan, *Atmos. Environ.*, 1997, **31**, 1953.

10 M. Kalberer, J. Yu, D. R. Cocker, R. C. Flagan and J. H. Seinfeld, *Environ. Sci. Technol.*, 2000, **34**, 4894.

11 E. O. Edney, D. J. Driscoll, W. S. Weathers, T. E. Kleindienst, T. S. Conver, C. D. Mc Iver and W. Li, *Aerosol Sci. Technol.*, 2001, **35**, 998.

12 A. Limbeck, M. Kulmala and H. Puxbaum, *Geophys. Res. Lett.*, 2003, **30**, DOI: 10.1029/2003GL017738.

13 Y. Iinuma, O. Böge, T. Gnauck and H. Herrmann, *Atmos. Environ.*, 2004, **38**, 761.

14 M. P. Tolocka, M. Jang, J. M. Ginter, F. J. Cox, R. M. Kamens and M. V. Johnston, *Environ. Sci. Technol.*, 2004, **38**, 1428.

15 M. Kalberer, D. Paulsen, M. Sax, M. Steinbacher, J. Dommen, A. S. H. Prévôt, R. Fisseha, V. Frankevich, R. Zenobi and U. Baltensperger, *Science*, 2004, **303**, 1659.

16 T. E. Kleindienst, T. S. Conver, C. D. Mc Iver and E. O. Edney, *J. Atmos. Chem.*, 2004, **47**, 79.

17 C. A. Koehler, J. D. Fillo, K. A. Ries, J. T. Sanchez and D. O. De Haan, *Environ. Sci. Technol.*, 2004, **38**, 5064.

18 R. J. Griffin, D. Dabdub and J. H. Seinfeld, *J. Geophys. Res.*, 2002, **107**, 4332.

19 S. N. Pandis, R. A. Harley, G. R. Cass and J. H. Seinfeld, *Atmos. Environ., Part A*, 1992, **26**, 2269.

20 M. Claeys, B. Graham, G. Vas, W. Wang, R. Vermeylen, V. Pashynska, J. Cafmeyer, P. Guyon, M. O. Andreae, P. Artaxo and W. Maenhaut, *Science*, 2004, **303**, 1173.

21 M. Claeys, W. Wang, A. C. Ion, I. Kourtchev, A. Gelencser and W. Maenhaut, *Atmos. Environ.*, 2004, **38**, 4093.

22 Hoffer, G. Kiss, M. Blazsó and A. Gelencsér, *Geophys. Res. Lett.*, 2004, **31**, L06115, DOI: 10.1029/2003GL018962.

23 N. Havers, P. Burba, J. Lambert and D. Klockow, *J. Atmos. Chem.*, 1998, **29**, 45.

24 S. Zappoli, A. Andracchio, S. Fuzzi, M. C. Facchini, A. Gelencsér, G. Kiss, Z. Krivácsy, Á. Molnár, E. Mészáros, H.-C. Hansson, K. Rosman and Y. Zebühr, *Atmos. Environ.*, 1999, **33**, 2733.

25 G. Kiss, B. Varga, I. Galambos and I. Ganszky, *J. Geophys. Res.*, 2002, **107**, 8339.

26 Z. Krivacsy, A. Gelencser, G. Kiss, E. Meszaros, A. Molnar, A. Hoffer, T. Meszaros, Z. Sarvari, D. Temesi, B. Varga, U. Baltensperger, S. Nyeki and E. Weingartner, *J. Atmos. Chem.*, 2001, **39**, 235.

27 D. Paulsen, J. Dommen, M. Kalberer, A. S. H. Prévôt, R. Richter, M. Sax, M. Steinbacher, E. Weingartner and U. Baltensperger, *Environ. Sci. Technol.*, 2005, **39**, 2668.

28 M. R. Alfarra, D. Paulsen, M. Gysel, A. A. Garforth, J. Dommen, A. S. H. Prévôt, D. R. Worsnop, U. Baltensperger and H. Coe, *Environ. Sci. Technol.*, 2004, submitted.

29 R. Fisseha, J. Dommen, M. Sax, D. Paulsen, M. Kalberer, R. Maurer, F. Höfler and U. Baltensperger, *Anal. Chem.*, 2004, **76**, 6535.

30 D. Paulsen, E. Weingartner, R. M. Alfarra and U. Baltensperger, *J. Aerosol. Sci.*, 2004, submitted.

31 M. Sax, R. Zenobi, U. Baltensperger and M. Kalberer, *Aerosol Sci. Technol.*, 2005, submitted.

32 M. R. Alfarra *et al.*, manuscript in preparation, 2005.

33 J. T. Jayne, D. C. Leard, X. Zhang, P. Davidovits, K. A. Smith, C. E. Kolb and D. R. Worsnop, *Aerosol Sci. Technol.*, 2000, **33**, 49.

34 D. R. Cocker, B. T. Mader, M. Kalberer, R. C. Flagan and J. H. Seinfeld, *Atmos. Environ.*, 2001, **35**, 6073.

35 J. D. Allan, J. L. Jimenez, H. Coe, K. N. Bower, P. I. Williams and D. R. Worsnop, *J. Geophys. Res.*, 2003, **108**, 4090.

36 F. W. McLafferty and F. Turecek, *Interpretation of Mass Spectra*, University Science Books, Mill Valley, CA, 1993.

37 H. Saathoff, K.-H. Naumann, M. Schnaiter, W. Schöck, O. Möhler, U. Schurath, E. Weingartner, M. Gysel and U. Baltensperger, *J. Aerosol Sci.*, 2003, **34**, 1297.

38 M. Gysel, E. Weingartner, S. Nyeki, D. Paulsen, U. Baltensperger, I. Galambos and G. Kiss, *Atmos. Chem. Phys.*, 2004, **4**, 35.

39 J. F. Pankow, *Atmos. Environ.*, 1994, **28**, 189.
40 B. K. Pun, S. Y. Wu, C. Seigneur, J. H. Seinfeld, R. J. Griffin and S. N. Pandis, *Environ. Sci. Technol.*, 2003, **37**, 3647.
41 B. Koo, A. S. Ansari and S. N. Pandis, *Atmos. Environ.*, 2003, **37**, 4757.
42 B. J. Turpin and J. J. Huntzicker, *Atmos. Environ., Part A*, 1991, **25**, 207.
43 P. E. Sheehan and F. M. Bowman, *Environ. Sci. Technol.*, 2001, **35**, 2129.
44 J. de Gouw, *8th International Global Atmospheric Chemistry Conference*, Christchurch, New Zealand, 2004.
45 J. R. Odum, T. Hoffmann, F. Bowman, D. Collins, R. C. Flagan and J. H. Seinfeld, *Environ. Sci. Technol.*, 1996, **30**, 2580.